MSI-78, an Analogue of the Magainin Antimicrobial Peptides, Disrupts Lipid Bilayer Structure via Positive Curvature Strain

Kevin J. Hallock,* Dong-Kuk Lee,*†‡ and A. Ramamoorthy*†‡
*Department of Chemistry, †Biophysics Research Division, and ‡Macromolecular Science and Engineering, University of Michigan, Ann Arbor, Michigan 48109-1055

ABSTRACT In this work, we present the first characterization of the cell lysing mechanism of MSI-78, an antimicrobial peptide. MSI-78 is an amphipathic α-helical peptide designed by Genaera Corporation as a synthetic analog to peptides from the magainin family. ^{31}P-NMR of mechanically aligned samples and differential scanning calorimetry (DSC) were used to study peptide-containing lipid bilayers. DSC showed that MSI-78 increased the fluid lamellar to inverted hexagonal phase transition temperature of 1,2-dipalmitoleoyl-phosphatidylethanolamine indicating the peptide induces positive curvature strain in lipid bilayers. ^{31}P-NMR of lipid bilayers composed of MSI-78 and 1-palmitoyl-2-oleoyl-phosphatidylethanolamine demonstrated that the peptide inhibited the fluid lamellar to inverted hexagonal phase transition of 1-palmitoyl-2-oleoyl-phosphatidylethanolamine, supporting the DSC results, and the peptide did not induce the formation of nonlamellar phases, even at very high peptide concentrations (15 mol %). ^{31}P-NMR of samples containing 1-palmitoyl-2-oleoyl-phosphatidylcholine and MSI-78 revealed that MSI-78 induces significant changes in the bilayer structure, particularly at high peptide concentrations. At lower concentrations (1–5%), the peptide altered the morphology of the bilayer in a way consistent with the formation of a toroidal pore. Higher concentrations of peptide (10–15%) led to the formation of a mixture of normal hexagonal phase and lamellar phase lipids. This work shows that MSI-78 induces significant changes in lipid bilayers via positive curvature strain and presents a model consistent with both the observed spectral changes and previously published work.

INTRODUCTION

Over the past few decades, numerous antimicrobial peptides have been isolated from a variety of different multicellular organisms including humans, frog, plants, and insects (Andreu and Rivas, 1998; Garcia-Olmedo et al., 1998). Antimicrobial peptides are an essential part of the innate immune system that provides protection against microbial invasion and many exhibit a broad spectrum of activity, destroying bacteria, protozoa, fungi, and/or viruses. Antimicrobial peptides are usually amphipathic and cationic, permeabilizing the cell membrane to cause the death of the pathogen. Because their mechanism differs from conventional antibiotics (Oren and Shai, 1998), they represent a unique option for countering the growing microbial resistance to traditional medicines. Unfortunately, most native peptides do not have the potency required to be pharmaceutically effective, but peptides designed for better efficacy may provide a viable treatment option (Maloy and Kari, 1995). The antibiotic peptide MSI-78 is an analog of magainin developed by Genaera Corporation.

MSI-78 is active against numerous bacterial strains, including strains that are resistant to conventional antibiotics (Maloy and Kari, 1995), but no details are currently known about the peptide's mechanism. MSI-78 is an analog of the naturally occurring antimicrobial peptides that comprise the magainin family, which was initially isolated from the frog *Xenopus laevis* (Zasloff, 1987). Magainin2 is thought to permeabilize cell membranes by forming toroidal-pores (Matsuzaki et al., 1998). Since MSI-78 was designed to be α-helical and amphipathic to mimic magainins (Maloy and Kari, 1995), we studied the peptide in lipid bilayers using ^{31}P-NMR and differential scanning calorimetry (DSC) to determine if MSI-78 operates by a similar mechanism. ^{31}P-NMR has been used to characterize lipids and their perturbation in many instances, including studies of peptide-induced changes in lipid phases (Gasset et al., 1988; Killian and de Kruijff, 1985; Keller et al., 1996; Fenske and Jarrell, 1991; Liu et al., 2001). However, many of these studies used multilamellar dispersions for their ^{31}P-NMR experiments, which complicate the analysis because of the broad, overlapping powder patterns resulting from mixtures of lipid phases. Mechanical alignment of the lipid bilayers circumvents this difficulty; it also increases spectral resolution and enhances the signal-to-noise ratio of the spectrum without any loss of information. Combining ^{31}P-NMR with DSC allows for a more complete understanding of peptide-induced curvature strain in the membrane since DSC is often used to characterize spontaneous membrane curvature. In this study, we report data consistent with MSI-78 operating via a toroidal pore mechanism similar to magainin2.

MATERIALS AND METHODS

Materials

DiPoPE, POPC, and POPE were purchased from Avanti Polar Lipids (Alabaster, AL). Chloroform and methanol were purchased from Aldrich

Submitted April 4, 2002, and accepted for publication December 4, 2002.
Address reprint requests to A. Ramamoorthy, Tel.: 734-647-6572; Fax: 734-764-8776; E-mail: ramamoor@umich.edu.

Abbreviations used: CSA, chemical shift anisotropy; DiPoPE, 1,2-dipalmitoleoyl-phosphatidylethanolamine; DSC, differential scanning calorimetry; H_I, normal hexagonal phase; H_{II}, inverted hexagonal phase; L_α, fluid lamellar phase; NMR, nuclear magnetic resonance spectroscopy; POPC, 1-palmitoyl-2-oleoyl-phosphatidylcholine; POPE, 1-palmitoyl-2-oleoyl-phosphatidylethanolamine.

0006-3495/03/05/3052/09 $2.00

Chemical (Milwaukee, WI). Naphthalene was purchased from Fisher Scientific (Pittsburgh, PA). All chemicals were used without further analysis or purification. MSI-78 is a 22-residue synthetic peptide with the amino acid sequence G-I-G-K-F-L-K-K-A-K-K-F-G-K-A-F-V-K-I-L-K-K-NH_2; it was designed, synthesized, and donated by Genaera Corporation.

Sample preparation

All mechanically aligned lipid samples used for NMR experiments were prepared using a naphthalene procedure published elsewhere (Hallock et al., 2002). Briefly, the membrane components were dissolved in an excess of 2:1 $CHCl_3$:CH_3OH (4 mg of lipids and an appropriate amount of peptide to produce the desired mole percentage). The lipid-peptide solution was dried under a stream of N_2 gas and redissolved in 2:1 $CHCl_3$:CH_3OH containing a 1:1 molar ratio of naphthalene to lipid-peptide. The solution was then dried on two thin glass plates (11 mm × 22 mm × 50 μm or 11 mm × 11 mm × 50 μm, Paul Marienfeld GmbH & Co., Bad Mergentheim, Germany). To remove the naphthalene and any residual organic solvent, the samples were vacuum dried for at least 6 h. After drying, the samples were indirectly hydrated in a sealed container with 93% relative humidity using a saturated $NH_4H_2PO_4$ solution (Washburn et al., 1926), for 1–2 days at 37°C, after which ~2 μL of H_2O was sprayed on the surface of the lipid-peptide film on the glass plates. The plates were stacked, wrapped with parafilm, sealed in plastic (Plastic Bagmart, Marietta, GA), and then equilibrated at 4°C for 1–2 days.

Solid-state NMR

All experiments were performed on a Chemagnetics/Varian Infinity 400 MHz solid-state NMR spectrometer operating at resonance frequencies of 400.14 MHz and 161.979 MHz for ^{1}H- and ^{31}P-nuclei, respectively. A built-in temperature control unit was used to maintain the sample's temperature; each sample was allowed to equilibrate at least 30 min before starting the experiment. Unless otherwise noted, experiments were performed at 30°C. The spectra of mechanically aligned samples were obtained using two home-built double resonance probes. One had a four turn square coil (14 mm × 14 mm × 4 mm) constructed from 2-mm wide flat wire with a spacing of 1 mm between turns and the other had a six-turn square coil (14 mm × 14 mm × 2 mm) made from the same material. A typical ^{31}P-90°-pulse length of 3.1 μs was used in both probes. Unless otherwise noted, all samples in the NMR probe were oriented with the lipid bilayer normal parallel to the external magnetic field of the spectrometer, which is defined as the parallel orientation. Some experiments were also performed on samples oriented with the bilayer normal perpendicular to the external magnetic field; this is referred to as the perpendicular orientation. The ^{31}P-chemical shift spectra were obtained using a spin-echo sequence (90°-τ-180°-τ, $\tau = 100$ μs) and a 40 kHz proton-decoupling RF field; the second half of the spin-echo was acquired. A 50-kHz ^{31}P-chemical shift spectral width and a recycle delay of 3 s were used. A typical spectrum required the co-addition of 100–1000 transients. The ^{31}P-spectra are referenced relative to 85% H_3PO_4 on thin glass plates (0 ppm). Data processing was accomplished using the software Spinsight (Chemagnetics/Varian) on a Sun Sparc workstation and IGOR 3.14 (Wavemetrics, Lake Oswego, OR) on a PC.

Differential scanning calorimetry

MSI-78 and DiPoPE were codissolved in a 2:1 $CHCl_3$:CH_3OH solution. The solution was dried under a stream of nitrogen, which was followed by drying under high vacuum for several hours. Enough buffer (10 mM Tris-HCl, 100 mM NaCl, 2 mM EDTA, pH = 7.4) was added to each sample to produce a 10 mg/ml lipid solution. The resultant solution was vortexed and then degassed. The fluid lamellar phase (L_α) to inverted hexagonal phase (H_{II}) transition temperature of the lipids was measured with a CSC 6100 Nano II Differential Scanning Calorimeter (Calorimetry Sciences, Provo, UT). The data were processed using the software provided by the manufacturer. The heating rate of all experiments was 1°C/min.

RESULTS

The effect of MSI-78 on membrane spontaneous curvature was studied by monitoring the peptide's ability to change the L_α-to-H_{II} phase transition temperature (T_H) of DiPoPE, a standard lipid used for these experiments (Epand and Epand, 2000; Wieprecht et al., 1997; Matsuzaki et al., 1998). The DSC thermograms of samples composed of DiPoPE combined with different concentrations of MSI-78 are shown in Fig. 1. Pure DiPoPE exhibited a T_H of 43.0°C. With the addition of peptide, the observed peak shifted to a higher temperature and broadened. At 0.2% peptide, T_H changed to 43.7°C and 0.4% peptide increased T_H further to 46.4°C. These data imply that MSI-78 induces positive curvature strain in lipid bilayers. Similar results were obtained from lipid bilayers containing magainin2 (Matsuzaki et al., 1998).

The L_α-to-H_{II} phase transition can also be monitored using ^{31}P-NMR of mechanically aligned samples. POPE bilayers undergo an L_α-to-H_{II} phase transition at 72°C. The ^{31}P-chemical shift spectrum shown in Fig. 2 *A* (*solid line*) was obtained from pure POPE bilayers at 30°C in the parallel orientation (bilayer normal parallel to the magnetic field); as expected, this sample exhibited a single peak at 28.8 ppm showing the sample is well aligned. The ^{31}P-NMR spectrum of the same sample at 30°C in the perpendicular orientation exhibited a single peak at −14.0 ppm (Fig. 2 *B*). As illustrated in Fig. 2, lipids in the parallel orientation have their main axis of rotation parallel to the external magnetic field (*right side* of Fig. 2 *A*), and in the perpendicular orientation, this rotational axis is perpendicular to the magnetic field (*right side* of Fig. 2 *B*). Because the lipids have only a single orientation with respect to the external magnetic field in both sample alignments, only one peak was observed in the ^{31}P-NMR spectra. When the sample was

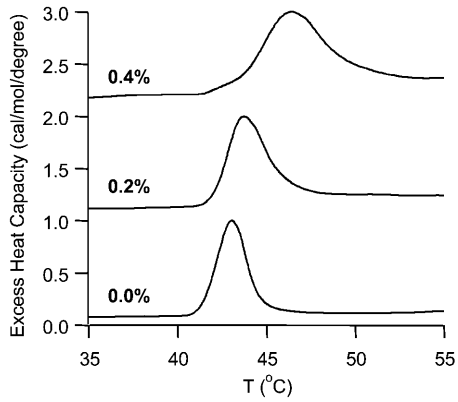

FIGURE 1 DSC thermograms of the L_α-to-H_{II} phase transition of DiPoPE at the listed concentrations of MSI-78. The phase transition temperature of DiPoPE (T_H) is 43°C. DiPoPE containing 0.2% MSI-78 exhibits a T_H of 43.7°C, and at 0.4% peptide the system has a T_H of 46.4°C.

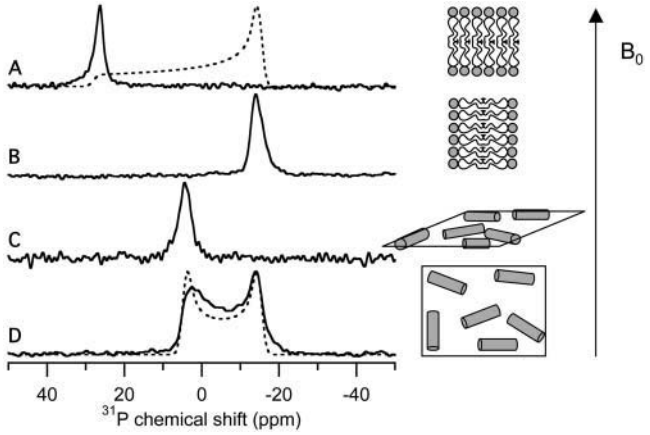

FIGURE 2 Experimental ^{31}P-chemical shift spectra of mechanically aligned samples of POPE at the specified orientation and temperature. Illustrations of the lipids and their orientation are also given. The magnetic field is represented by the arrow and labeled B_0. (*A*) Parallel orientation at 30°C (*solid line*); simulated ^{31}P-chemical shift powder pattern using the following chemical shift values: $\sigma_{\parallel} = 28$ ppm and $\sigma_{\perp} = -15$ ppm (*dashed line*). (*B*) Perpendicular orientation at 30°. (*C*) Parallel orientation at 80°C. (*D*) Perpendicular orientation at 80°C (*solid line*); simulated spectrum (*dashed line*) assuming a circular distribution of hexagonal phase tubes using the following chemical shift values: $\sigma_{\parallel} = -15$ ppm and $\sigma_{\perp} = 4.4$ ppm (*dashed line*).

heated to 80°C, which is above the L_{α}-to-H_{II} phase transition temperature, POPE in the H_{II} phase exhibited a single peak at 4.5 ppm in the parallel orientation (Fig. 2 *C*), but when the sample was rotated by 90° to the perpendicular orientation, the ^{31}P-NMR spectrum of H_{II} phase lipids had a chemical shift span of ~20 ppm (Fig. 2 *D*, *solid line*). The reason these spectra differ from spectra of L_{α} phase lipids is that the H_{II} phase tubes form between adjacent bilayers and therefore the aligned bilayers result in the formation of H_{II} phase tubes in a plane parallel to the surface of the glass plates as illustrated on the right side of Fig. 2 *C*. In the parallel orientation, all of these tubes have their tubular axis perpendicular to the external magnetic field and exhibit the same NMR frequency. When the sample is turned 90° to the perpendicular direction, the axes of the tubes are randomly distributed in two dimensions relative to the external magnetic field (shown on the *right side* in Fig. 2 *D*), which results in the ^{31}P-spectrum shown in Fig. 2 *D*. The observed lineshape is indicative of two-dimensional disorder within the mechanically aligned hexagonal phase sample (Fig. 2 *D*) and can be simulated assuming a circular distribution (Moll and Cross, 1990). If the tubes were randomly arranged in three dimensions, a typical powder pattern would have been observed (Thayer and Kohler, 1981). Fig. 2 *D* compares the simulated spectrum assuming a circular distribution (*dashed line*) and the experimental spectrum obtained from the POPE sample in a perpendicular orientation at 80°C (*solid line*).

To probe the effect of MSI-78 on POPE, ^{31}P-NMR experiments at 30° were performed at peptide concentrations ranging from 1–15%. The observed ^{31}P-chemical shift spectra were found to be relatively independent of peptide concentration. At 0% peptide, there was a single peak at 28.8 ppm (Fig. 3 *A*). The addition of 1% peptide shifted the intense peak to 27 ppm, but changed little else (Fig. 3 *B*). The inclusion of 3% MSI-78 moved the main peak to 24.8 ppm, and a low intensity peak centered at 16.0 ppm was also present (Fig. 3 *C*). Increasing the peptide's concentration to 5% had little additional effect, with the tallest peak at 25.0 ppm and the low intensity peak at 16.4 ppm (Fig. 3 *D*). Doubling the peptide concentration to 10% yielded a spectrum (Fig. 3 *E*) that was similar to the 3% and 5% peptide samples. Surprisingly, increasing the concentration of the peptide to 15% resulted in only one additional change: the appearance of a small peak at –0.8 ppm indicative of an isotropic phase (Fig. 3 *F*). In most of the ^{31}P-spectra of POPE samples containing peptide, there was a low intensity peak near 17 ppm (Fig. 3, *C–F*). To determine whether MSI-78 inhibits the L_{α}-to-H_{II} phase transition of POPE, samples containing 1% and 10% peptide concentrations were heated to 75°C, above the L_{α}-to-H_{II} phase transition temperature. Fig. 4 shows the ^{31}P-chemical shift spectra of mechanically aligned POPE bilayers containing 1% MSI-78, acquired at 30°C (Fig. 4 *A*) and 75°C (Fig. 4 *B*). The 30°C sample had an intense peak at 27 ppm, but when the temperature was increased to 75°C, the only significant intensity was at 4.7 ppm (Fig. 4 *B*), which is similar to the ^{31}P-NMR spectra observed from pure POPE bilayers at comparable orientation and temperatures (compare Fig. 4 with Fig. 2, *A* and *C*). Based on this, we conclude that the presence of 1% MSI-78 does not significantly inhibit the L_{α}-to-H_{II} phase transition of POPE bilayers. However, this phase

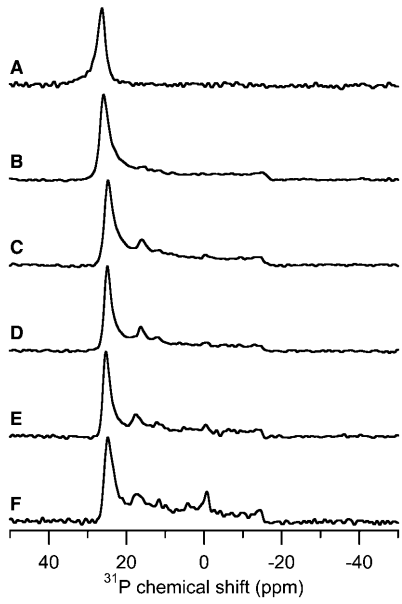

FIGURE 3 Experimental ^{31}P-chemical shift spectra of POPE bilayers containing different concentrations of MSI-78. Concentrations are listed in mole percent and the experiments were performed at 30°C. The samples were aligned parallel to the magnetic field. (*A*) 0% MSI-78, (*B*) 1% MSI-78, (*C*) 3% MSI-78, (*D*) 5% MSI-78, (*E*) 10% MSI-78, and (*F*) 15% MSI-78.

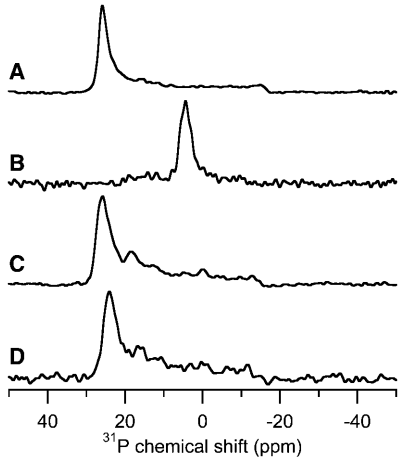

FIGURE 4 Experimental ^{31}P-chemical shift spectra of POPE bilayers containing 1% MSI-78. The samples were aligned parallel to the magnetic field. (*A*) 1% MSI-78 at 30°C, (*B*) 1% MSI-78 at 75°C, (*C*) 10% MSI-78 at 30°C, and (*D*) 10% MSI-78 at 75°C.

transition was prevented by the inclusion of 10% MSI-78 in POPE bilayers (Fig. 4, *C–D*). The 10% peptide sample in POPE at 30°C is shown in Fig. 4 *C* and the most intense peak was at 25.8 ppm. However at 75°C, the main peak shifted to 24.1 ppm and no peak indicating hexagonal phase formation (4–5 ppm) was observed (Fig. 4 *D*). The prevention of the formation of H_{II} is consistent with MSI-78 inducing positive curvature strain in lipid bilayers and inhibiting the formation of inverted phases, in agreement with the DSC data.

Fig. 5 shows the effect of increasing concentrations of MSI-78 on bilayers composed of POPC. The changes induced by

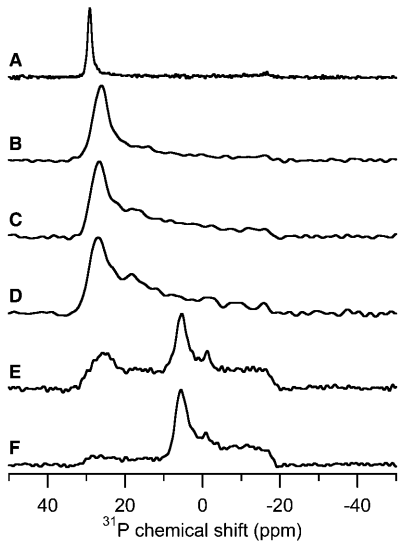

FIGURE 5 Experimental ^{31}P-chemical shift spectra of POPC bilayers containing different concentrations of MSI-78. Concentrations are listed in mole percent and the experiments were performed at 30°C. The samples were aligned parallel to the magnetic field. (*A*) 0% MSI-78, (*B*) 1% MSI-78, (*C*) 3% MSI-78, (*D*) 5% MSI-78, (*E*) 10% MSI-78, and (*F*) 15% MSI-78.

MSI-78 in POPC bilayers were more pronounced than the minimal variation observed in POPE bilayers (Fig. 3). Without any peptide (Fig. 5 *A*), pure POPC bilayers align well, evidenced by the single peak near 30 ppm. At 1% peptide (Fig. 5 *B*), the most intense peak shifted to 26.1 ppm and a broad component appeared, extending between 27 ppm and –18 ppm. With 3% MSI-78 present (Fig. 5 *C*), the location of the most intense peak changed little (26.7 ppm), but the broad component increased in relative intensity. A similar change occurred when the concentration of peptide was increased to 5% (Fig. 5 *D*). The lineshape of the broad component is unusual. It is not a typical powder pattern (Fig. 2 *A*, *dashed line*) nor is it indicative of a circular distribution (Fig. 2 *D*). The gradually decreasing intensity from 27 ppm to –18 ppm indicates the presence of a different orientational distribution of the lipids. As will be shown later in this paper, this lineshape can be accounted for by a toroidal distribution of the lipids. At 10% peptide (Fig. 5 *E*), the observed ^{31}P-chemical shift spectrum changed considerably. The most intense peak was found at 5.3 ppm with a general broad component extending from 30 to –18 ppm and a low intensity peak centered at 25.8 ppm. The 25.8-ppm peak suggests that some of the lipids remained parallel to the magnetic field while the 5.3-ppm peak indicates that the high concentration of peptide induced the formation of another lipid phase, which will be discussed in greater detail later. The spectrum of 15% MSI-78 in POPC (Fig. 5 *F*) was similar to that of the 10% sample, although the intensity in the chemical shift range of 30 ppm to 6 ppm decreased significantly. At 10% and 15% MSI-78 in POPC (Fig. 5, *E* and *F*), a peak near –1 ppm was also present in the ^{31}P-spectra, suggesting the formation of an isotropic phase at high peptide concentrations.

DISCUSSION

MSI-78 is an α-helical, antimicrobial analog of the magainin family of peptides. The DSC data (Fig. 1) and the variable temperature ^{31}P-NMR data (Fig. 4) show that MSI-78 induces positive curvature strain in lipid bilayers similar to magainin2, a member of the magainin family of antimicrobial peptides (Matsuzaki et al., 1998). With this in mind, it is not surprising that MSI-78 induced more changes in the ^{31}P-spectra of samples composed of POPC than in those containing POPE. The former is more susceptible to positive curvature strain than the latter because phosphatidylcholine headgroups are larger than phosphatidylethanolamine headgroups (Janes, 1996).

At low concentrations (1–5%), the ^{31}P-spectra of peptide-containing POPC bilayers exhibited unusual lineshapes. These lineshapes reflect the orientational distribution of the lipid headgroups in the sample, but the spectra observed from the samples are not a typical lineshape, i.e, of a lamellar phase, hexagonal phase, isotropic phase, or crystalline powder distribution; some other distribution must be present to generate this lineshape. Because of the structural similarities

between MSI-78 and magainin2, a reasonable hypothesis is that MSI-78 forms toroidal pores (Fig. 6 *A*) similar to magainin2 (Matsuzaki et al., 1998). To simulate a ^{31}P-spectrum expected from lipids in any distribution, the angular dependence of the observed chemical shift (σ_{obs}) and its distribution (or shape factor) must be known. For a rigid powder sample, the former is expressed by

$$\sigma_{obs} = \sigma_{33}\cos^2\theta + \sigma_{22}\sin^2\theta\sin^2\phi + \sigma_{33}\sin^2\theta\cos^2\phi, \quad (1)$$

while the latter is

$$\sin\theta\, d\theta. \quad (2)$$

In Eqs. 1 and 2, σ_{ii} ($i = 1,2,3$) are the principal components of the chemical shielding tensor, θ is the angle between σ_{33} and the external magnetic field (B_0), and ϕ is the angle between σ_{11} and the projection of B_0 onto the σ_{11}–σ_{22} plane. For lipids in a fluid phase,

$$\sigma_{obs} = \sigma_{\parallel}\cos^2\theta + \sigma_{\perp}\sin^2\theta. \quad (3)$$

After some straightforward algebra (Stewart, 1991), the shape factor for a torus was determined to be

$$b(a+b) - b^2\sin\theta\, d\theta. \quad (4)$$

In Eq. 3, $\sigma_{\parallel}$ and $\sigma_{\perp}$ are the tensor components parallel and perpendicular to the lipids main axis of rotation, respectively. The angle θ is the same as above, b is the thickness of the lipid monolayer, and a is the radius of the pore at its smallest diameter as shown in Fig. 6 *B*. To evaluate this model, we assumed the thickness of the peptide-containing bilayer was the same as a bilayer composed solely of POPC, which is ~40 Å (Vogel et al., 2000; Marsh, 1990). We also assumed that the toroidal pore produced by MSI-78 has a diameter of 20 Å, similar to the pore produced by magainin2 (Matsuzaki et al., 1998). These postulates result in $b = 20$ Å and $a = 10$ Å. It should be noted that for a toroidal distribution, Eqs. 3 and 4 are only valid for the parallel and perpendicular sample orientations; more complex equations are required for other sample orientations, but these equations are beyond the scope of this present study.

Using these values, the ^{31}P-chemical shift spectra of lipids distributed in the form of a torus were simulated (Fig. 7 *A*, *dashed line*) and compared with the 5% MSI-78 in POPC sample (Fig. 7 *A*, *solid line*). The simulation qualitatively mimics the features of the experimental spectrum, notably the decreasing intensity from high frequency to low frequency that is not modeled by other standard distributions (compare with Fig. 2, *dashed lines*). However, the experimental and simulations are not identical. In Fig. 7 *A*, the experimental spectrum has less intensity near –15 ppm and a low-intensity peak at 18 ppm, which are both absent from the simulation. The former might be caused by the presence of peptides in the pore; peptides presumably displace many of the lipids near the center of the pore (Fig. 6 *A*), reducing the number of lipids perpendicular to the magnetic field resulting in a reduction of intensity near –15 ppm. We also adjusted the values of a and b to determine the dependence of the lineshape on these variables. For example, when the radius of the pore (a) is reduced to 5Å, the simulation has less intensity near the perpendicular edge of the spectrum (Fig. 7 *B*, *dashed line*). Increasing the value of a has the opposite effect. An adjustment in the value of length of the lipid (b) also changes the simulated spectrum, with larger b values intensifying the parallel edge of the spectrum (simulations not shown).

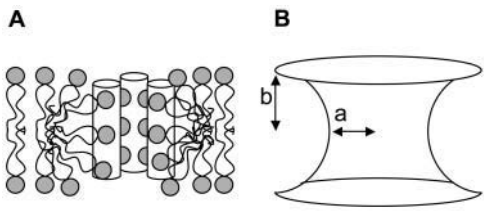

FIGURE 6 *A* and *B* illustrate the toroidal-pore model of magainin, similar to Fig. 9 in Matsuzaki et al. (1998). (*A*) Magainin is illustrated using a cylinder, with the gray spheres representing the headgroups of the lipids. The lines represent the lipid's acyl chains. (*B*) The length of a lipid monolayer, b, and the radius of the pore at its narrowest location, a, characterize the toroidal pore.

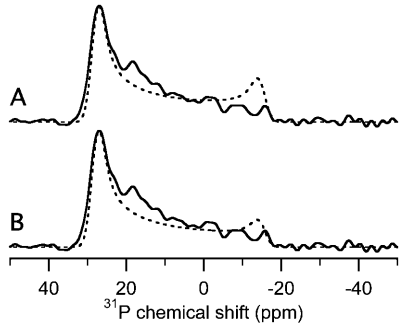

FIGURE 7 The comparison of the experimental 5% MSI-78 in POPC (Fig. 5 *C*) spectrum (*solid line*) with simulated spectra (*dashed line*). The parameters used for the simulations were $\sigma_{\parallel} = 28$ ppm, $\sigma_{\perp} = -15$ ppm, and line broadening of 1.5 ppm. Using the notation of Fig. 6, the simulations used (*A*) $b = 20$ Å and $a = 10$ Å, and (*B*) $b = 20$ Å and $a = 5$ Å. The experiments were performed at 30°C.

Before proceeding further, the caveats of the above toroidal pore model need to be discussed. The above simulations were generated with three assumptions: 1), all of the lipids within the sample are participating in toroidal pore formation; 2), the motion of lipids through the toroidal pore is slow on the NMR timescale; and 3), the orientation of the ^{31}P-CSA tensor and motional axis are relatively unchanged in the presence of peptide. To determine if the first assumption is acceptable, we need to ascertain how many lipids compose a pore by approximating the surface area of the toroidal pore. The surface area of the inside portion of a torus can be obtained by integrating Eq. 4, which yields

$$2\pi^2 b(a+b) - 4\pi b^2, \quad (5)$$

or a surface area of ≈6800 Å^2 for a toroidal pore with b = 20 Å and a = 10 Å. If we assume that POPC has a cross-sectional area of 65 Å^2 (Marsh, 1990; Funari et al., 1997), the surface area of a toroidal pore equals that of 105 lipids. Although it is not known how many peptides are required for the formation of a single pore, a reasonable estimate is five monomers per toroidal pore (Matsuzaki et al., 1998). Each peptide occupies a surface area equal to ≈3 lipids, suggesting that ~90 lipids participate in the formation of each toroidal pore. Therefore, 90% of the lipids are expected to participate in pore formation at 5% peptide concentration, demonstrating that the assumption of 100% participation is reasonable.

Regarding the second assumption, if the lipids were moving rapidly on the NMR timescale, an average peak would be observed between 12 and 20 ppm (depending on pore size). In the above spectra, low-intensity peaks in this range were observed in POPE bilayers containing MSI-78 (Fig. 3) and POPC bilayers containing low concentrations of MSI-78 (most notably Fig. 5 *D*). The combination of a low-intensity peak and an intense broad component suggests a small percentage of lipids are moving rapidly across the bilayer on the NMR timescale while the majority are in toroidal pore structures that are moving slowly. This variation might be caused by a distribution of pore structures, with some pores stable on the NMR timescale and others not. Additional investigation is required to better understand this phenomenon, but based on the observed relative spectral intensity, the majority of lipids are static on the NMR timescale.

Considering the third assumption, the possibility of a change in the ^{31}P-CSA and/or motional axis of the lipid leading to the observed lineshapes in Fig. 5 cannot be excluded (Thayer and Kohler, 1981), but we consider it improbable. It seems unlikely that the presence of peptide would significantly alter the ^{31}P-CSA in POPC bilayers without causing similar changes in the CSA of POPE bilayers (compare Fig. 5 with Fig. 3). If headgroup reorientation occurred, the observed ^{31}P-CSA span would have changed (Thayer and Kohler, 1981) and the span did not change significantly as shown in Fig. 5; only the spectral lineshapes were altered by the presence of peptide. In conclusion, the toroidal model is consistent with the observed lineshapes, but it is not the only possible explanation; another possibility is the peptide inducing a mosaic spread in the aligned bilayer sample. This possibility will be discussed after the high concentration peptide samples are considered.

When the concentration of MSI-78 is 10% in POPC bilayers (Fig. 5 *E*), a peak at 5.3 ppm is present that is similar to the 4.5-ppm peak originating from H_{II} phase lipids observed in samples of pure POPE at 80°C (Fig. 2 *C*). However, the DSC data (Fig. 1) and ^{31}P-NMR (Fig. 4) demonstrate that MSI-78 induces positive curvature strain, which is inconsistent with the peptide-induced formation of H_{II}. But, lipids in an H_I phase would produce an identical peak, and the formation of H_I would be consistent with MSI-78 inducing positive curvature strain. Instead of a different lipid phase, the 5.3-ppm peak could also represent a peptide-induced conformational/orientational change in the lipids (Noggle et al., 1982). In this hypothesis, the lipids remain in an L_α bilayer, but the orientation of the lipid headgroup has changed. The nature of the L_α phase dictates that a single peak is observed in both the parallel and perpendicular directions as shown in Fig. 2, *A* and *B*, respectively. However, the ^{31}P-chemical shift spectrum of 10% MSI-78 in POPC in the perpendicular orientation rules out this possibility. Fig. 8 shows the ^{31}P-chemical shift spectrum of 10% MSI-78 peptide in POPC sample in the parallel (Fig. 8 *A*, *solid line*) and perpendicular (Fig. 8 *B*, *solid line*) orientations. A single peak was not observed in the perpendicular orientation, eliminating the possibility that the 5.3-ppm peak was caused by the lipids uniformly adopting a different orientation. In fact, Fig. 8 *B* has a lineshape similar to the spectrum obtained from H_{II} phase lipids in the perpendicular sample orientation (Fig. 2 *D*, *solid line*). However, Fig. 8 *B* has significantly more intensity near −15 ppm because the 10% MSI-78 in POPC sample contains multiple components, most likely a combination of lipids in toroidal pores and H_I phase. To simulate the spectra shown in Fig. 8, the relative percentages of the components must be determined. The two phases are easily distinguished in Fig. 8 *A* because the components exhibit excellent resolution in the parallel orientation. Fig. 8 *A* can be simulated assuming 73% of the lipids are in toroidal pores and the other 27% are in an H_I phase (Fig. 8 *A*, *dashed line*). Using the same percentages of both phases, the perpendicular orientation was also fit (Fig. 8 *B*, *dashed line*). These simulations demonstrate that the ^{31}P-spectra of high concentrations MSI-78 in POPC induce changes in lipid bilayers consistent with the presence of toroidal pores and H_I phase lipids, but this is not an exclusive explanation. As was mentioned previously, a large mosaic spread could cause the observation of lineshape ascribed to toroidal pores.

In terms of aligned bilayers, mosaic spread refers to a macroscopic disorder in the stacking of the bilayers leading

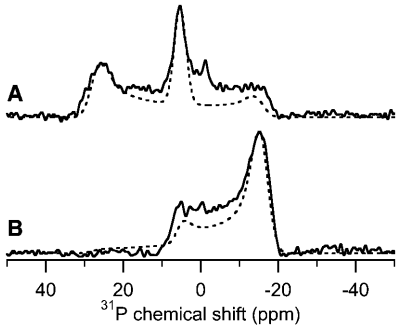

FIGURE 8 Experimental and simulated ^{31}P-chemical shift spectra of POPC bilayers containing 10% MSI-78. (*A*) Parallel orientation, (*B*) perpendicular orientation. The best-fitting simulations combined lipids in toroidal pores (73%) and H_I phase (27%). The spectral parameters for the simulation of the toroidal pore component: $\sigma_{\|} = 26$ ppm, $\sigma_{\perp} = -15$ ppm, 2 ppm line broadening; for the H_I phase component, $\sigma_{\|} = -15$ ppm, $\sigma_{\perp} = +5.3$ ppm, and 1.5 ppm line broadening. The experiments were performed at 30°C.

to a distribution of bilayer orientations with respect to the external magnetic field. Even though a mechanically aligned sample with a large mosaic spread could account for some of the spectral lineshapes reported in this paper, DSC and NMR experiments presented here demonstrate that MSI-78 induces positive curvature strain in lipid bilayers (Figs. 1 and 4) and that the peptide induces the formation of an aligned H_I phase at high concentrations (Fig. 8). Because of this, it is reasonable to assume that the peptide induces the formation of a structure in between an L_α phase and the H_I phase at intermediate concentrations. Consider the scheme shown in Fig. 9: without any peptide, the lipids form aligned bilayers (Fig. 9 *A*). With the addition of a low concentration of MSI-78, the ^{31}P-NMR spectra suggest that the lipids either induce a mosaic spread (Fig. 9 *B*) or the formation of toroidal pores (Fig. 9 *C*) in the sample. At high peptide concentrations, the peptide induces the formation of an aligned H_I phase (Fig. 9 *D*). It seems unlikely the peptide would induce a large mosaic spread at low concentrations and an aligned hexagonal phase at high concentrations; this route is shown in the top scheme (Fig. 9 $A \rightarrow 9\ B \rightarrow 9\ D$). The bottom scheme (Fig. 9 $A \rightarrow 9\ C \rightarrow 9\ D$), which includes toroidal pores as an intermediate structure, is similar to a mechanism proposed for L_α-to-H_{II} phase transitions (Siegel, 1999). Aligned toroidal pores could be an intermediate step in formation of an aligned H_I phase, which is why we consider it more likely for toroidal pores to be present in the samples that were studied than a peptide-induced mosaic spread.

The structure of the proposed peptide-induced H_I phase is not known, but it may be similar to the illustration shown in Fig. 10 *A*. In this model, the peptides are end-to-end with a peptide-lipid structure similar to that of a toroidal pore (Fig. 6 *A*). In the absence of information about the peptide's orientation, it is possible that the peptide intercalates between lipid headgroups, tilting them away from the peptide with the lipid's acyl chains tilt inward, filling the space beneath the peptide as shown in Fig. 10 *B*. In this case, the lipids along the sides of the peptide would be tilted significantly more than the lipids at the end of the helix. Additional investigation is currently underway to better characterize the nature of the peptide-induced H_I phase.

Compared to the peptide-induced changes discussed above, relatively small changes were observed in bilayers composed of POPE (Fig. 3). Despite the low intensity, these changes can be interpreted in a context similar to the changes observed in POPC bilayers, i.e., toroidal pore formation in POPE bilayers. The appearance of a low-intensity peak at 16.4 ppm is consistent with lipids moving through a toroidal pore rapidly on the NMR timescale as previously mentioned (Fig. 3, *C–F*). There is also the presence of a low-intensity broad component in all peptide-containing POPE bilayers reminiscent of the toroidal pore intensity described above in detail (Fig. 3, *B–F*). Another similarity between these two types of bilayers is the isotropic phase that was found at high peptide concentrations (Fig. 3 *F*). This peak could indicate the presence of peptide-lipid micelles or a peptide-induced cubic phase. Our data cannot distinguish between these possibilities and further experiments would be required to clarify the nature of this minor component. These spectra suggest that MSI-78 induces similar toroidal pores in both POPE and POPC, but the peptide is less disruptive of POPE bilayers and does not induce the formation of an H_I phase even at 15% peptide concentration. Initially, it may seem unusual for an antibacterial peptide to be less effective against phosphatidylethanolamine lipids, an important component of bacterial membranes, but this is not the first time such an observation has been reported. Similar results were reported for magainin2, which is more effective at causing leakage from membranes containing phosphatidylcholine lipids than phosphatidylethanolamine lipids (Matsuzaki et al., 1998).

Before concluding, the biological relevance of using high peptide concentrations and zwitterionic membranes to study antimicrobial peptides needs to be discussed. High peptide concentrations are not required for antimicrobial activity; in fact, only micromolar concentrations of MSI-78 or magainin2 are necessary to inhibit bacterial growth (Maloy and

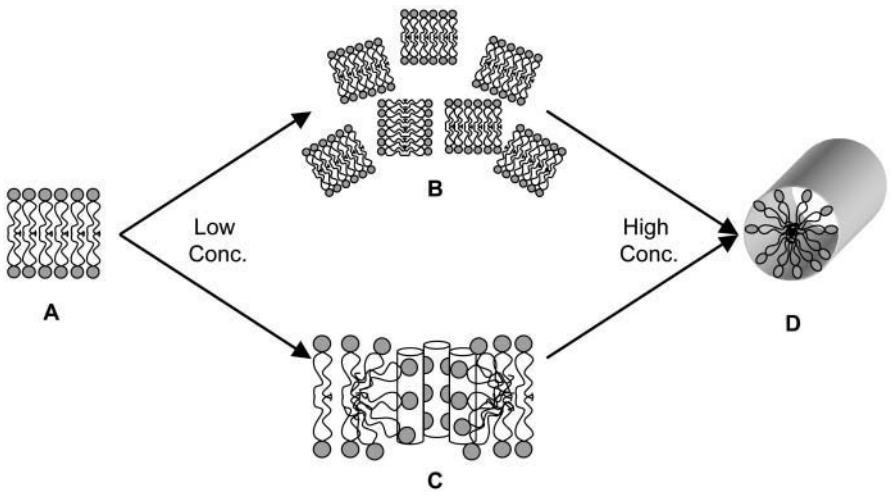

FIGURE 9 Possible transitional schemes of the peptide-induced hexagonal formation due to increasing peptide concentrations. (*A*) L_α phase lipids, (*B*) L_α phase lipids with a large mosaic spread, (*C*) Lipids in a peptide-induced toroidal pore, and (*D*) Lipids in the H_I phase. Peptides are omitted in *B* and *D* just for clarity.

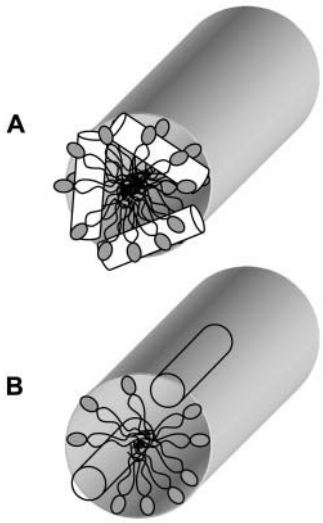

FIGURE 10 Illustrations of the peptide-induced normal hexagonal phase. (*A*) An extension of the toroidal pore mechanism. (*B*) The peptide (represented by the cylinders) intercalates between the lipid headgroups, tilting the lipids.

Kari, 1995), although total cell lysis is not observed until magainin2 reaches concentrations of 10% (Matsuzaki et al., 1997). But, minimum inhibitory concentrations measure the concentration of the peptide in bulk solution, not near the surface of the bacterial membrane, or more importantly, the ratio of peptide to lipid during pore formation. This latter event is poorly understood. Peptide association or aggregation and peptide-lipid complex formation is required to form the pore (Matsuzaki, 1998; Oren and Shai, 1998; Andreu and Rivas, 1998). Currently, little information is available about the peptide-to-lipid ratio in the pre-pore complex or during pore formation, but concentration of peptide is expected to be higher than micromolar. In an effort to gain insight into these transient pore-forming species, high concentrations of peptide were used to mimic the high concentrations of peptide likely to be present in the pre-pore and pore complexes.

In this work, the effect of MSI-78 on bilayers composed of zwitterionic lipids was studied, not the peptide's effect on bilayers containing both zwitterionic and anionic lipids which more closely mimic bacterial membranes. Although it has been shown that anionic lipids attract cationic peptides to the lipid-water interface and are an essential selection filter for antimicrobial peptides, anionic lipids are not essential for the binding of cationic peptides such as magainin2 and PGLa to lipid bilayers (Dathe and Wieprecht, 1999; Wieprecht et al., 2000; Bechinger et al., 1993). In fact, Wieprecht and coworkers demonstrated that if the magainins are assumed to be initially present in the lipid-water interface, then ''magainins would bind distinctly better to neutral than to charged membranes'' (Wieprecht et al., 1999). In the mechanically aligned bilayers used throughout this work, bulk water is absent from the samples, thus eliminating the need for long-range electrostatic interactions to induce peptide aggregation near the bilayer surface; in other words, the peptides are always at the lipid-water interface and the presence of anionic lipids is not required for peptide interaction with the bilayer. The changes reported in this manuscript verify that MSI-78 interacts with lipid bilayers in the absence of anionic lipids.

CONCLUSION

This article constitutes the first characterization of the membrane disrupting mechanism of MSI-78, a designed peptide analog of the magainin peptides. Using both DSC and variable temperature ^{31}P-NMR experiments, the results presented here establish that MSI-78 induces substantial changes in lipid bilayers via positive curvature strain. In bilayers composed of POPC, unusual ^{31}P-NMR spectra were obtained from mechanically aligned samples containing 1–5% peptide. These spectra were found to be consistent with the formation of toroidal pores similar to the pores formed by magainin2. At higher peptide concentrations, the formation of a peptide-induced H_I phase was observed in POPC bilayers. To the best of our knowledge, this is the first time a peptide-induced H_I phase has been reported. Similar but less pronounced effects were observed in bilayers composed of POPE. Additional work is currently underway in our laboratory to further characterize MSI-78, including investigation of the peptide's effect on bilayers containing more than one type of lipid. These results add to the body of knowledge concerning the mechanism of antimicrobial peptides and may aid in the design of more potent peptide pharmaceuticals.

We thank Katherine Henzler Wildman for useful discussions. We thank Dr. Lee Maloy, Genaera Corporation, for donating the MSI-78 peptide that made this work possible. We also thank Dr. Timothy Cross and the reviewers for their valuable comments on this work.

This research was supported by research funds from the National Science Foundation (CAREER development award to A.R.). K.J.H. was supported by the National Institutes of Health-Michigan Molecular Biophysics Training Program (GM08270).

REFERENCES

Andreu, D., and L. Rivas. 1998. Animal antimicrobial peptides: an overview. *Biopolymers*. 47:415–433.

Bechinger, B., M. Zasloff, and S. J. Opella. 1993. Structure and orientation of the antibiotic peptide magainin in membranes by solid-state nuclear magnetic resonance spectroscopy. *Protein Sci.* 2:2077–2084.

Dathe, M., and T. Wieprecht. 1999. Structural features of helical antimicrobial peptides: their potential to modulate activity on model membranes and biological cells. *Biochim. Biophys. Acta Biomembr.* 1462: 71–87.

Epand, R. M., and R. F. Epand. 2000. Modulation of membrane curvature by peptides. *Biopolymers*. 55:358–363.

Fenske, D. B., and H. C. Jarrell. 1991. ^{31}P-two-dimensional solid-state exchange NMR—application to model membrane and biological systems. *Biophys. J.* 59:55–69.

Funari, S. S., C. DiVitta, and G. Rapp. 1997. X-ray diffraction and NMR studies on mixtures of non-ionic surfactant (C12EO2) and phospholipids (POPC). *Acta Phys. Pol. A*. 91:953–960.

Garcia-Olmedo, F., A. Molina, J. M. Alamillo, and P. Rodriguez-Palenzuela. 1998. Plant defense peptides. *Biopolymers*. 47:479–491.

Gasset, M., J. A. Killian, H. Tournois, and B. de Kruijff. 1988. Influence of cholesterol on gramicidin-induced H_{II} phase formation in phosphatidylcholine model membranes. *Biochim. Biophys. Acta*. 939: 79–88.

Hallock, K. J., K. Henzler Wildman, D. K. Lee, and A. Ramamoorthy. 2002. An innovative procedure using a sublimable solid to align lipid bilayers for solid-state NMR studies. *Biophys. J*. 82:2499–2503.

Janes, N. 1996. Curvature stress and polymorphism in membranes. *Chem. Phys. Lipids*. 81:133–150.

Keller, S. L., S. M. Gruner, and K. Gawrisch. 1996. Small concentrations of alamethicin induce a cubic phase in bulk phosphatidylethanolamine mixtures. *Biochim. Biophys. Acta Biomembr*. 1278:241–246.

Killian, J. A., and B. de Kruijff. 1985. Importance of hydration for gramicidin-induced hexagonal-H_{II} phase formation in dioleoylphosphatidylcholine model membranes. *Biochemistry*. 24:7890–7898.

Liu, F., R. Lewis, R. S. Hodges, and R. N. McElhaney. 2001. A differential scanning calorimetric and P-31 NMR spectroscopic study of the effect of transmembrane alpha-helical peptides on the lamellar-reversed hexagonal phase transition of phosphatidylethanolamine model membranes. *Biochemistry*. 40:760–768.

Maloy, W. L., and U. P. Kari. 1995. Structure-activity studies on magainins and other host defense peptides. *Biopolymers*. 37:105–122.

Marsh, D. 1990. CRC Handbook of Lipid Bilayers. CRC Press, Boca Raton, FL. pp. 387.

Matsuzaki, K. 1998. Magainins as paradigm for the mode of action of pore forming polypeptides. *Biochim. Biophys. Acta*. 1376:391–400.

Matsuzaki, K., K. Sugishita, M. Harada, N. Fujii, and K. Miyajima. 1997. Interactions of an antimicrobial peptide, magainin 2, with outer and inner membranes of Gram-negative bacteria. *Biochim. Biophys. Acta*. 1327: 119–130.

Matsuzaki, K., K. Sugishita, N. Ishibe, M. Ueha, S. Nakata, K. Miyajima, and R. M. Epand. 1998. Relationship of membrane curvature to the formation of pores by magainin 2. *Biochemistry*. 37:11856–11863.

Moll, F. D., and T. A. Cross. 1990. Optimizing and characterizing alignment of oriented lipid bilayers containing gramicidin D. *Biophys. J*. 57: 351–362.

Noggle, J. H., J. F. Marecek, S. B. Mandal, R. Vanvenetie, J. Rogers, M. K. Jain, and F. Ramirez. 1982. Bilayers of phosphatidyldiacylglycerol and phosphatidylcholesterol give ^{31}P-NMR spectra characteristic for hexagonal and isotropic phases. *Biochim. Biophys. Acta*. 691:240–248.

Oren, Z., and Y. Shai. 1998. Mode of action of linear amphipathic alpha-helical antimicrobial peptides. *Biopolymers*. 47:451–463.

Siegel, D. P. 1999. The modified stalk mechanism of lamellar/inverted phase transitions and its implications for membrane fusion. *Biophys. J*. 76:291–313.

Stewart, J. 1991. Calculus. Brooks/Cole Publishing Company, Pacific Grove, CA.

Thayer, A. M., and S. J. Kohler. 1981. Phosphorus-31 nuclear magnetic resonance spectra characteristic of hexagonal and isotropic phospholipid phases generated from phosphatidylethanolamine in the bilayer phase. *Biochemistry*. 20:6831–6834.

Vogel, M., C. Munster, W. Fenzl, and T. Salditt. 2000. Thermal unbinding of highly oriented phospholipid membranes. *Phys. Rev. Lett*. 84:390–393.

Washburn, E. W., C. J. West, and C. Hull. 1926. International Critical Tables of Numerical Data, Physics, Chemistry, and Technology. Published for the National Research Council by McGraw-Hill, New York.

Wieprecht, T., O. Apostolov, M. Beyermann, and J. Seelig. 2000. Membrane binding and pore formation of the antibacterial peptide PGLa: thermodynamic and mechanistic aspects. *Biochemistry*. 39:442–452.

Wieprecht, T., M. Beyermann, and J. Seelig. 1999. Binding of antibacterial magainin peptides to electrically neutral membranes: thermodynamics and structure. *Biochemistry*. 38:10377–10387.

Wieprecht, T., M. Dathe, R. M. Epand, M. Beyermann, E. Krause, W. L. Maloy, D. L. MacDonald, and M. Bienert. 1997. Influence of the angle subtended by the positively charged helix face on the membrane activity of amphipathic, antibacterial peptides. *Biochemistry*. 36:12869–12880.

Zasloff, M. 1987. Magainins, a class of antimicrobial peptides from *Xenopus* skin: isolation, characterization of two active forms, and partial cDNA sequence of a precursor. *Proc. Natl. Acad. Sci. USA*. 84:5449–5453.